Stephens, R.D.; Warner, B.D. (2020). "Main-belt Asteroids Observed from CS3: 2019 July to September." *Minor Planet Bull.* **47**, 50-60.

Vecchione, A.; Noschese, A.; Catapano, A. (2018). "Lightcurve Analysis and Rotation Period for (140158) 2001 SX169." *Minor Planet Bull.* **45**, 183-184.

VizieR (2021). *http://vizier.u-strasbg.fr/viz-bin/VizieR*

Warner, B.D.; Harris, A.W.; Pravec, P. (2009). "The Asteroid Lightcurve Database." *Icarus* **202**, 134-146. Updated 2021 June. *http://www.minorplanet.info/lightcurvedatabase.html*

Warner, B.D. (2012). The MPO Users Guide: A Companion Guide to the MPO Canopus/PhotoRed Reference Manuals. BDW Publishing, Colorado Springs, CO.

Warner, B.D.; Stephens, R.D.; Harris, A.W. (2013). "(1727) Mette." *CBET* **3402**.

Warner, B.D. (2014). "Asteroid Lightcurve Analysis at CS3-Palmer Divide Station: 2014 January-March." *Minor Planet Bull.* **41**, 144-155.

Warner, B.D. (2018a). MPO Canopus software, version 10.7.11.3. *http://www.bdwpublishing.com*

Warner, B.D. (2018b). "Near-Earth Asteroid Lightcurve Analysis at CS3-Palmer Divide Station: 2017 October-December." *Minor Planet Bull.* **45**, 138-147.

Waszczak, A.; Chang, C.-K.; Ofek, E.O.; Laher, R.; Masci, F.; Levitan, D.; Surace, J.; Cheng, Y.-C.; Ip, W.-H.; Kinoshita, D.; Helou, G.; Prince, T.A.; Kulkarni, S. (2015). "Asteroid Light Curves from the Palomar Transient Factory Survey: Rotation Periods and Phase Functions from Sparse Photometry." *Astron. J.* **150**, A75.

Wisniewski, W.Z.; McMillan, R.S. (1987). "Differential CCD Photometry of Faint Asteroids in Crowded Star Fields and Nonphotometric Sky Conditions." *Astron. J.* **93**, 1264.

Wisniewski, W.Z.; Michalowski, T.M.; Harris, A.W.; McMillan, R.S. (1997). "Photometric Observations of 125 Asteroids." *Icarus* **126**, 395-449.

LIGHTCURVES OF SEVEN ASTEROIDS

Eric V. Dose
3167 San Mateo Blvd NE #329
Albuquerque, NM 87110
mp@ericdose.com

(Received: 2021 October 13)

We present lightcurves, synodic rotation periods, and G value (H-G) estimates for seven asteroids.

We present asteroid lightcurve photometry results obtained by following the workflow process described by Dose (2020a), with later improvements (Dose, 2020b). This workflow applies to each image an ensemble of typically 20-60 nearby ATLAS refcat2 catalog (Tonry et al, 2018) comparison ("comp") stars as a basis for asteroid photometry. Diagnostic plots and numerous comp stars allow for effective identification and removal of outlier, variable, and poorly measured comp stars.

The custom workflow produces a time series of asteroid magnitude estimates on Sloan r' (SR) catalog basis, unreduced and without H-G adjustment. These magnitudes are imported directly into *MPO Canopus* software (Warner, 2018, version 10.8.4.11) where they are adjusted for distances and phase-angle dependence, fit by Fourier analysis including identifying and ruling out of aliases, and plotted. Phase-angle dependence is corrected with a H-G model, using the *G* value that minimizes fit RMS error across all nights' data.

No nightly zero-point adjustments (DeltaComps in *MPO Canopus* terminology) were made to any session herein, other than by adjusting the G value (H-G phase model). All lightcurve data herein have been submitted to ALCDEF.

Lightcurve Results

Seven asteroids were observed from Deep Sky West observatory (IAU V28) at 2210 meters elevation in northern New Mexico. Images were acquired with a 0.35-meter SCT reduced to f/7.7; a SBIG STXL-6303E camera cooled to -35 C and fitted with a Clear filter (Astrodon); and a PlaneWave L-500 mount. The equipment was operated remotely via ACP software (DC-3 Dreams, version 8.3), running plan files generated for each night by the author's python scripts (Dose, 2020a). Observations often cycled among 2-4 asteroids. Exposure times targeted 5-8 millimagnitudes uncertainty in asteroid instrumental magnitude, subject to a minimum of 120 seconds to ensure suitable comp-star photometry, and to a maximum of 900 seconds. All exposures were autoguided.

FITS images were plate-solved by *PinPoint* (DC-3 Dreams) or *TheSkyX* (Software Bisque) and were calibrated using temperature-matched, median-averaged dark images and recent flat images of a flux-adjustable flat panel. Every photometric image was visually inspected; all images with poor tracking, obvious interference by cloud or moon, or having stars or other light sources within 10 arcseconds of the target asteroid were excluded. Photometry-ready images that pass these screens were submitted to the workflow, which applies separately measured second-order transforms from Clear filter to deliver asteroid magnitudes in Sloan r' passband.

In this work, "period" refers to an asteroid's synodic rotation period, and "SR" denotes the Sloan r' passband.

666 Desdemona. This relatively bright inner main-belt asteroid was found to have synodic rotation period 14.612±0.004 hours, in agreement with two previous reports (14.607 h, Marciniak et al, 2015; 14.5995 h, Pál et al, 2020), but differing from others (15.45 h, Stephens, 2001; 9.6 h, Behrend 2004web, Behrend 2005web, and Behrend 2006web).

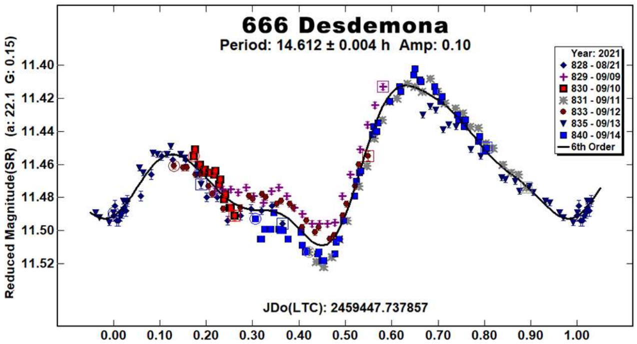

Fourier fit to the present data has RMS error of 7 millimagnitudes and indicates a G value (H-G phase model) close to 0.15. The period spectrum disfavors 15.45 h and 9.6 h candidate solutions, neither of which is an obvious alias of the present solution.

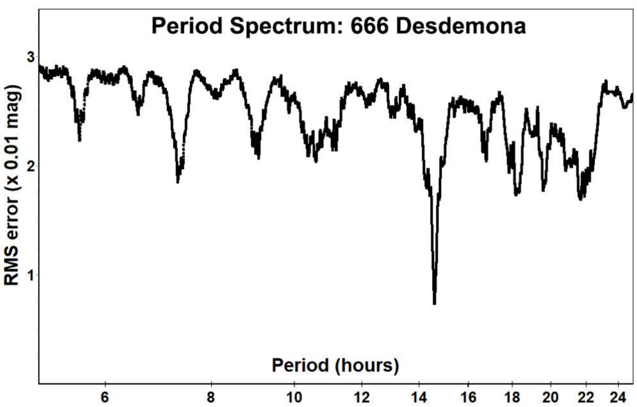

903 Nealley. This outer main-belt asteroid was found to have a rotational period of 58.032±0.024 h, at wide variance from previous reports (21.60 h, Warner, 2004; 19.72 h or 19.58 h, Warner, 2012; 16.2 h, Behrend, 2020web; 28.9882 h, Pál et al, 2020). Fourier fit to the present data has RMS error of 11 millimagnitudes and is optimized at G value of 0.08.

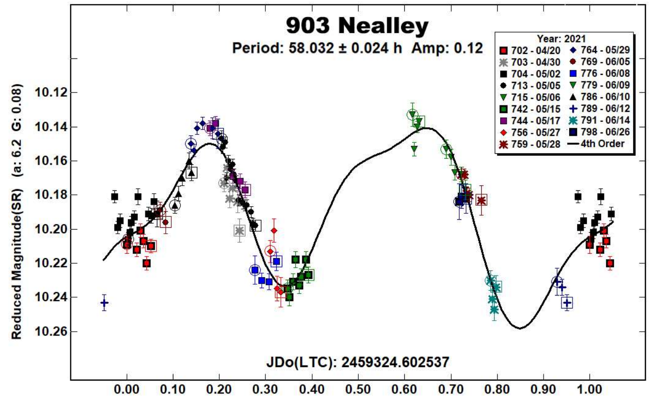

Even with 17 nights' observations, lightcurve phase coverage was incomplete. Even so, the period spectrum does not support periods shorter than about 26 hours. The coverage gap at present phases of 0.40 to 0.58 allows for a possible monomodal period of 29.016 h, which would agree with the result of Pál et al, but the present data slightly favor the 58.032 h bimodal period. The other previously reported periods are not readily explained as aliases of these monomodal or bimodal period candidates.

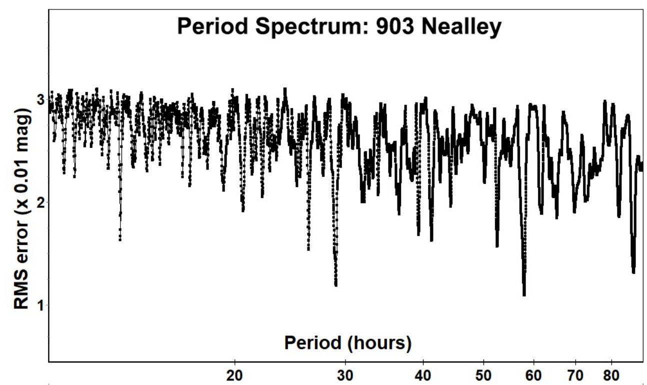

904 Rockefellia. This outer main-belt asteroid was found to have rotation period of 6.822±0.002 h, in agreement with both determinations by Polakis (6.826 h, Polakis, 2018; 6.82 h, Polakis, 2020) but at variance with other previous reports (4.93 h, Koff, 2004web; 14.04 h, Behrend, 2009web; 5.823 h, Fauvaud and Fauvaud, 2013; 14.04 h, Behrend, 2014web; and 14.038 h, Behrend, 2020web). Our Fourier fit has RMS error of 8 millimagnitudes and suggests G of 0.08.

Number	Name	yyyy mm/dd	Phase	L_{PAB}	B_{PAB}	Period(h)	P.E.	Amp	A.E.	Grp
666	Desdemona	2021 08/21-09/14	21.9,12.3	9	6	14.612	0.004	0.10	0.02	MB-I
903	Nealley	2021 04/20-06/26	6.5,17.4	195	9	58.032	0.024	0.12	0.03	MB-O
904	Rockefellia	2021 09/16-10/05	4.4,9.9	348	9	6.822	0.002	0.14	0.02	MB-O
1990	Pilcher	2021 08/06-08/26	*7.3,4.4	327	3	2.841	0.001	0.13	0.02	FLOR
3932	Edshay	2021 09/03-09/08	15.5,13.7	10	12	3.431	0.001	0.33	0.02	EUN
4826	Wilhelms	2021 03/29-08/07	*21.7,28.9	238	20	15.004	0.002	0.84	0.04	PHO
7328	Casanova	2021 08/21-09/11	20.5,11.2	6	-1	9.122	0.002	0.46	0.03	EUN

Table I. Observing circumstances and results. The phase angle is given for the first and last date. If preceded by an asterisk, the phase angle reached an extrema during the period. L_{PAB} and B_{PAB} are the approximate phase angle bisector longitude/latitude at mid-date range (see Harris et al., 1984). Grp is the asteroid family/group (Warner et al., 2009).

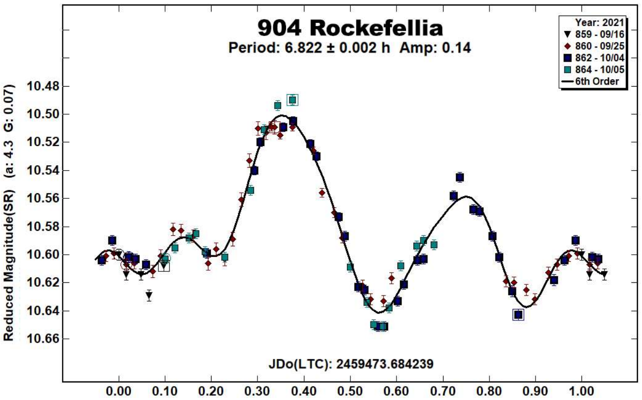

The other, previously reported period candidates are neither supported by the present period spectrum, nor readily explained as aliases of the present solution. The second-best solution in the period spectrum is simply twice the period proposed here.

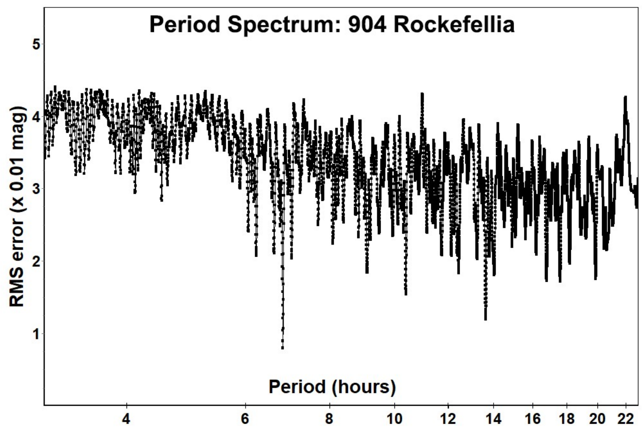

1990 Pilcher. Only one previous report exists of rotational period for this Flora asteroid; it is listed in the LCDB as ambiguous, between 3.895 h and 2.842 h (Brincat and Grech, 2017). We confirm the latter with a new report of period 2.8410±0.0005 h. Our Fourier fit has RMS error of 10 millimagnitudes and suggests G of 0.20.

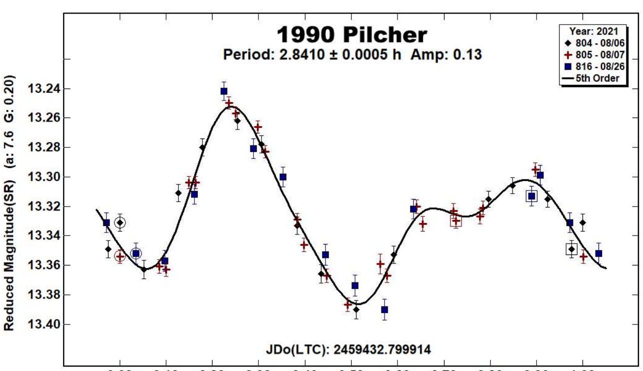

Our period spectrum benefited from two periods' coverage on the second night; it does not support the 3.895 h period candidate.

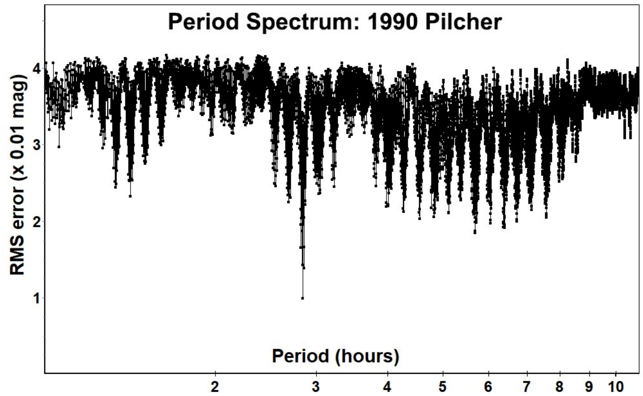

3932 Edshay. We report a rotational period of 3.431±0.001 h for this Eunomia asteroid, confirming both previous reports (3.432 h, Waszczak et al, 2015; 3.444 h, Behrend, 2017web). The lightcurve is clearly bimodal. Our Fourier fits yielded RMS error of 7 millimagnitudes and G value of 0.05.

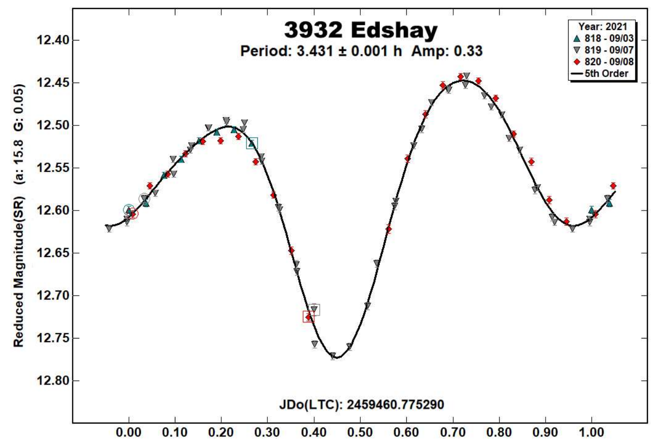

4826 Wilhelms. For this Phocaea asteroid, we find a rotational period of 15.004±0.002 h and a large amplitude of 0.84 magnitudes, in disagreement with the sole known previous report of 54 h (Pravec et al., 2012web). Our Fourier fit has RMS error of 47 millimagnitude. G value is approximately 0.45.

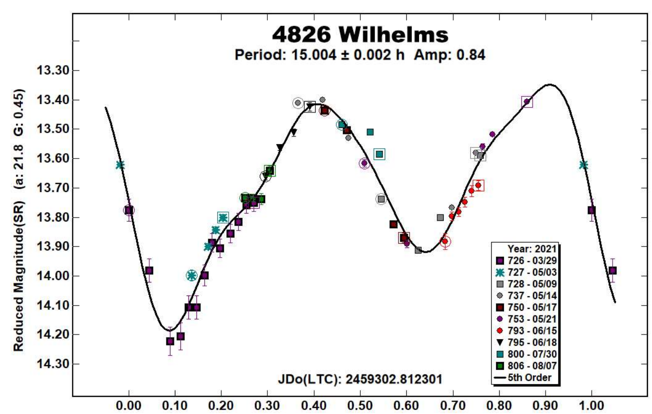

Despite 10 nights' observations over 18 weeks, the period spectrum remains noisy - signals do appear for periods of 2 and 2.5 times our report of 15.004 h, and we cannot rule these out, although the lightcurve shape at our proposed period is entirely reasonable. Our spectrum does, however, strongly disfavor the candidate period of 54 hours.

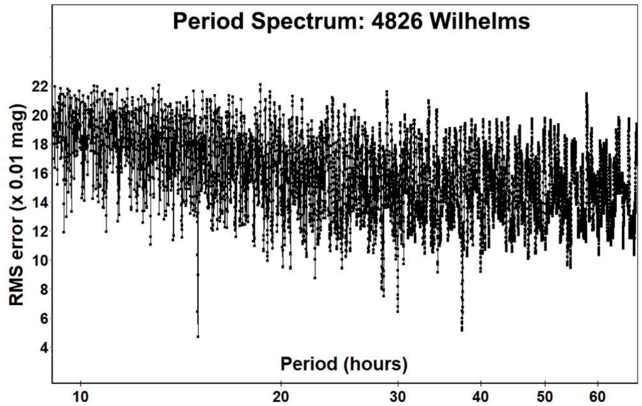

7328 Casanova. For this Eunomia asteroid, we confirm the sole known previous period report of 9.122 h (Waszczak et al, 2015) with our own finding of 9.122±0.002 h. Our Fourier fits yielded RMS error of 18 millimagnitudes and G of 0.25.

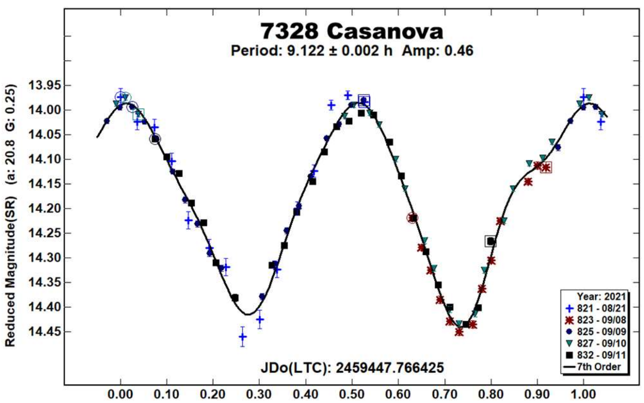

Acknowledgements

The author thanks all authors of the ATLAS paper (Tonry et al, 2018) and its numerous contributors for providing without cost the ATLAS refcat2 catalog release. This project makes extensive use of the python language interpreter and of several supporting packages (notably: pandas, ephem, matplotlib, requests, astropy, and statsmodels), all provided without cost.

References

Behrend, R. (2004web, 2005web, 2006web, 2009web, 2014web, 2017web, 2020web). Observatoire de Genève web site. *http://obswww.unige.ch/~behrend/page_cou.html*

Brincat, S.M.; Grech, W. (2017). "Photometric Observations of Main-Belt Asteroids 1990 Pilcher and 8443 Svecica." *Minor Planet Bull.* **44**, 287-288.

Dose, E. (2020a). "A New Photometric Workflow and Lightcurves of Fifteen Asteroids." *Minor Planet Bull.* **47**, 324-330.

Dose, E. (2020b). "Lightcurves of Nineteen Asteroids." *Minor Planet Bull.* **48**, 69-76.

Fauvaud, S.; Fauvaud, M. (2013). "Photometry of Minor Planets. I. Rotation Periods from Lightcurve Analysis for Seven Main-Belt Asteroids." *Minor Planet Bull.*, **40**, 224-229.

Harris, A.W.; Young, J.W.; Scaltriti, F.; Zappalà, V. (1984). "Lightcurves and phase relations of the asteroids 82 Alkmene and 444 Gyptis." *Icarus* **57**, 251-258.

Koff, R.A. (2004web). Posting on the CALL web site. *https://minplanobs.org/MPInfo/php/callsearch.php*

Marciniak, A. and 23 colleagues (2015). "Against the biases in spins and shapes of asteroids." *Planetary Space Sci.*, **118**, 256-266.

Pál, A.; Szakáts, R.; Kiss, C.; Bódi, A.; Bognár, Z.; Kalup, C.; Kiss, L.L.; Marton, G.; Molnár, L.; Plachy, E.; Sárneczky, K.; Szabó, G. M.; Szabó, R. (2020). "Solar System Objects Observed with TESS - First Data Release: Bright Main-belt and Trojan Asteroids from the Southern Survey." *Astrophys. J. Suppl. Series* **247**, 26.

Polakis, T. (2018). "Lightcurve Analysis for Eleven Main-Belt Asteroids." *Minor Planet Bull.*, **45**, 199-203.

Polakis, T. (2020). "Photometric Observations of Twenty-Seven Minor Planets." *Minor Planet Bull.*, **47**, 314-321.

Pravec, P.; Wolf, M.; Sarounova, L. (2012). Ondrejov Asteroid Photometry Project. *http://www.asu.cas.cz/~ppravec/newres.txt*

Stephens, R.D. (2001). "Rotational Periods and Lightcurves of 1277 Dolores, 666 Desdemona, and (7505) 1997 AM2." *Minor Planet Bull.* **28**, 28-29.

Tonry, J.L.; Denneau, L.; Flewelling, H.; Heinze, A.N.; Onken, C.A.; Smartt, S.J.; Stalder, B.; Weiland, H.J.; Wolf, C. (2018). "The ATLAS All-Sky Stellar Reference Catalog." *Astrophys. J.* **867,** A105, 1-16.

Warner, B.D. (2004). "Lightcurve Analysis for Numbered Asteroids 863, 903, 907, 928, 977, 1386, 2841, and 75747." *Minor Planet Bull.* **31**, 85-88.

Warner, B.D.; Harris, A.W.; Pravec, P. (2009). "The asteroid lightcurve database." *Icarus*, **202**, 134-146. Updated 2020 August. *http://www.minorplanet.info/lightcurvedatabase.html*

Warner, B.D. (2012). "Asteroid Lightcurve Analysis at the Palmer Divide Observatory: 2011 June - September." *Minor Planet Bull.* **39**, 16-21.

Warner, B.D. (2018). MPO Canopus Software, version 10.8.4.11, BDW Publishing. *http://www.bdwpublishing.com*

Waszczak, A.; Chang, C.-K.; Ofek, E.O.; Laher, R.; Masci, F.; Levitan, D.; Surace, J.; Cheng, Y.-C.; Ip, W.-H.; Kinoshita, D.; Helou, G.; Prince, T.A.; Kulkarni, S. (2015). "Asteroid Light Curves from the Palomar Transient Factory Survey: Rotation Periods and Phase Functions from Sparse Photometry." *Astron. J.* **150**, 75.